Electronic Supplementary Material (ESI) for Nanoscale Horizons.
This journal is © The Royal Society of Chemistry 2023

Supporting Information

Local Control of Au/MoS_2 Schottky Barrier by Top ZnO Nanowire Gate for High-Performance Photodetection

Yu Xiao[1], Guisheng Zou[1], Jinpeng Huo[1], Tianming Sun[1,2], Jin Peng[1], Zehua Li[1], Daozhi Shen[3], Lei Liu[1,]*

[1] Department of Mechanical Engineering, State Key Laboratory of Tribology, Key Laboratory for Advanced Manufacturing by Materials Processing Technology, Ministry of Education of PR China, Tsinghua University, Beijing 100084, P. R. China

[2] College of Materials Science and Engineering, Taiyuan University of Technology, Taiyuan 030024, Shanxi Province, China

[3] Institute for Quantum Computing, Department of Chemistry, Centre for Advanced Materials Joining, University of Waterloo, Waterloo, Ontario, N2L 3G1 Canada

* Corresponding author. E-mail address: liulei@tsinghua.edu.cn

Table of Contents

I. Supplementary Figures

1. Detailed fabrication processes

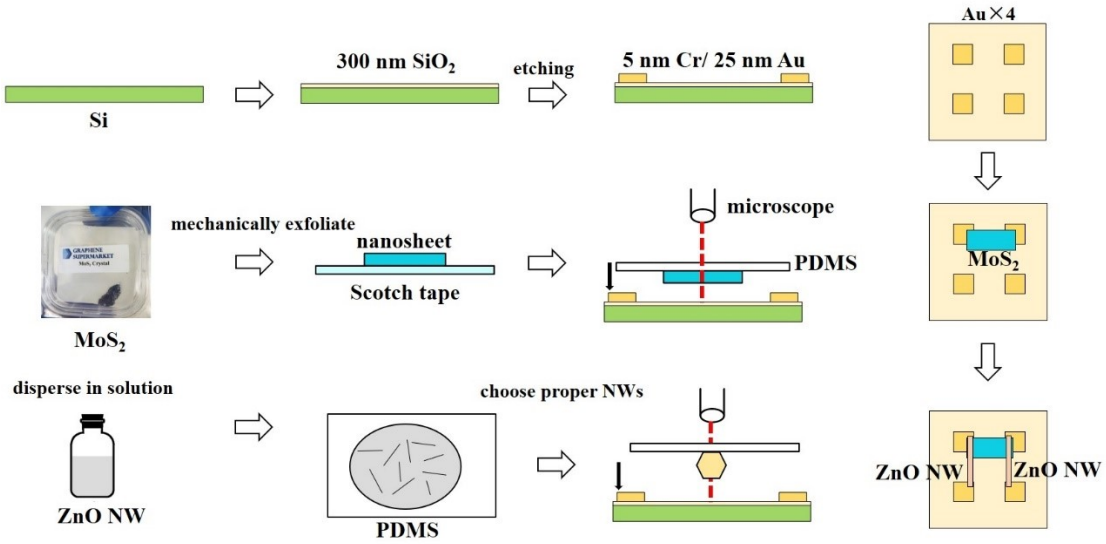

Figure S1. The fabrication process of the MoS_2 device with ZnO nanowire gates.

2. The diameter of the left ZnO

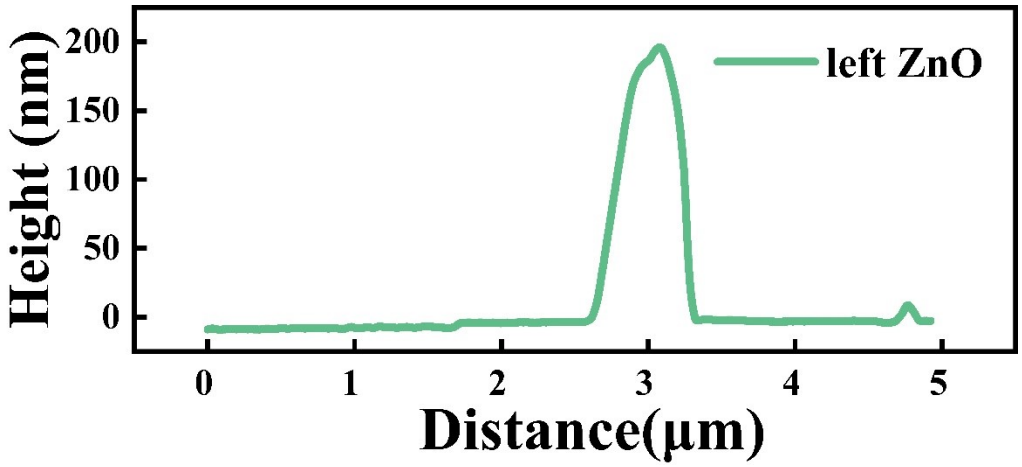

Figure S2. The diameter of the left ZnO in Figure 1b using AFM testing

3. Detailed Raman test positions

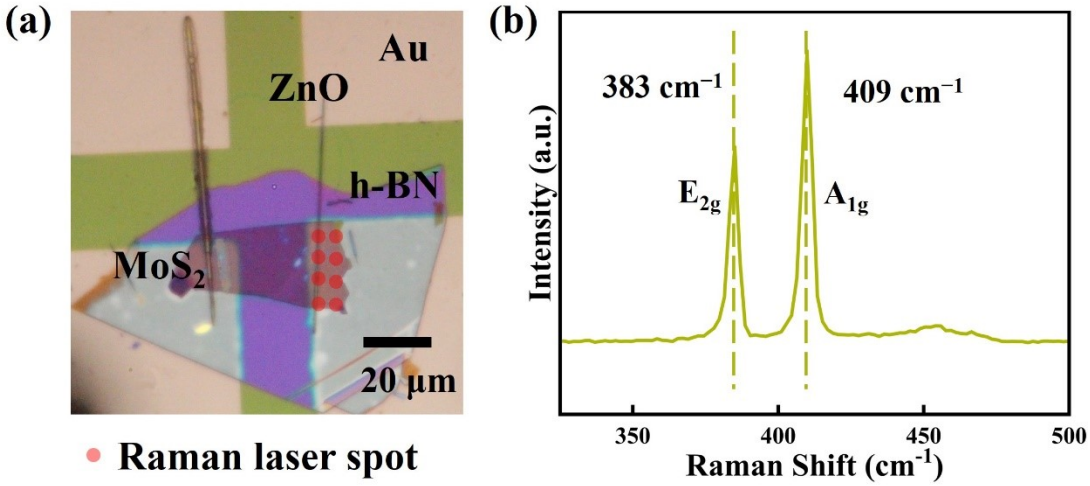

Figure S3. Detailed Raman test positions in the NG device. (a) An 1 um Raman spot is focused at eight locations in the red regions, and the right ZnO nanowire cross through the left four detection spots. (b) The eight results are the same, and no peaks of ZnO appear in the Raman tests.

4. Comparison between the photodetecting areas and the device

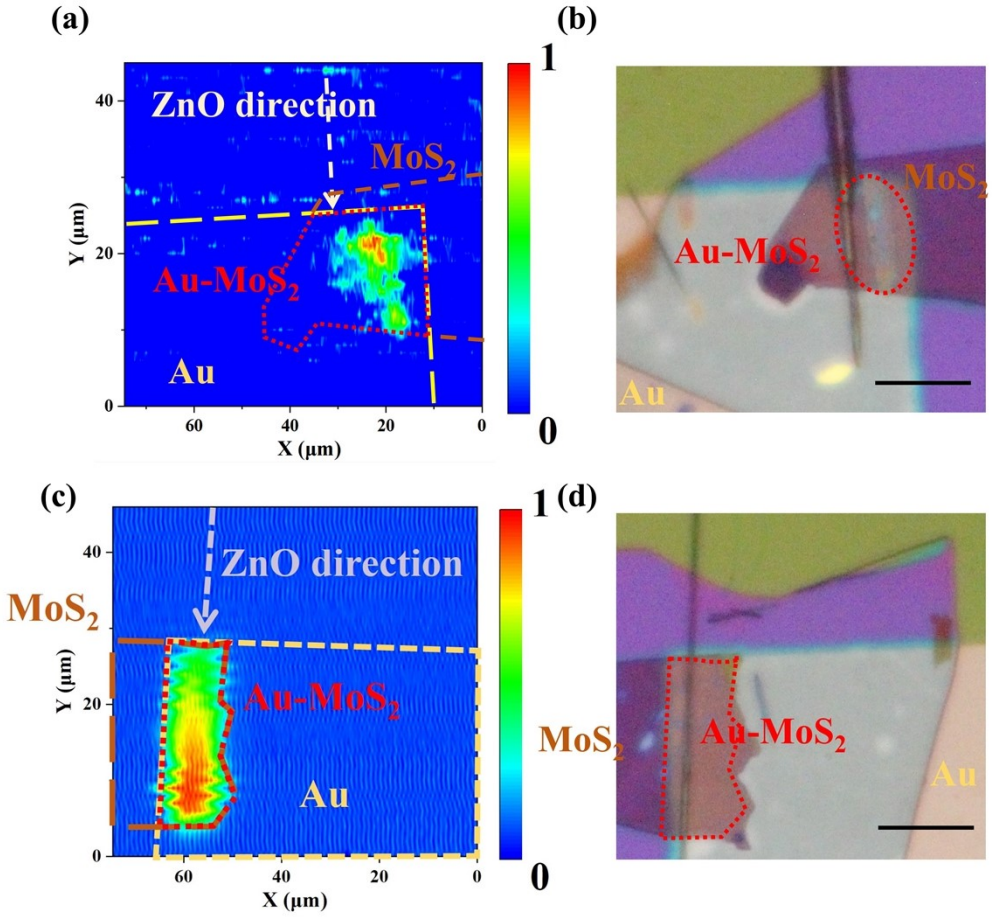

Figure S4. Photo-mapping of the Au-MoS_2 structure on both sides. (a) The normalized photodetecting intensity on the left side. (b) The corresponding optical image of Au-MoS_2 on the left side. (c) The normalized photodetecting intensity on the right side. (d) The corresponding optical image of Au-MoS_2 on the right side. Scale bar: 20 μm.

5. The supplementary photodetecting performances of Au-MoS_2 Schottky junction

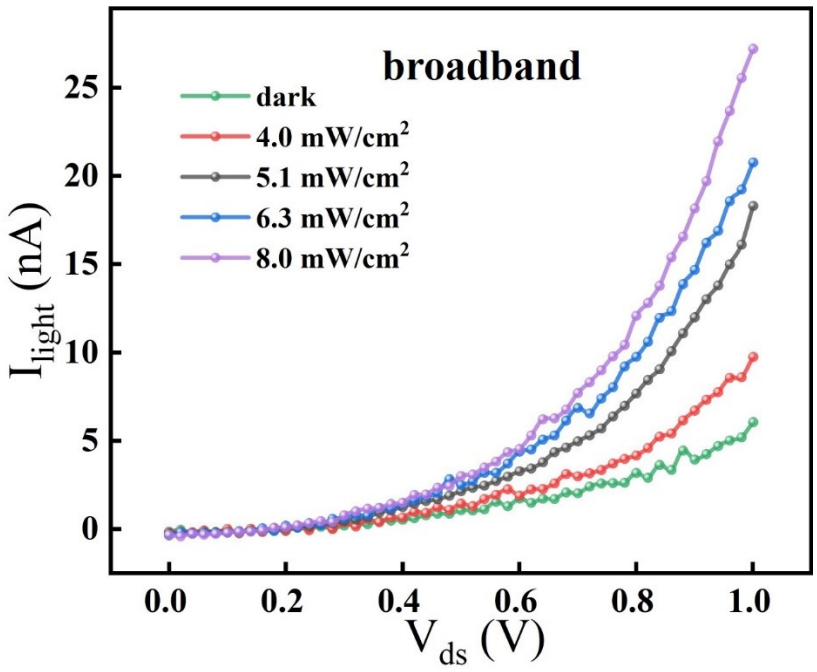

Figure S5. The photodetecting performances of Au-MoS_2 Schottky junction under a broadband halogen light.

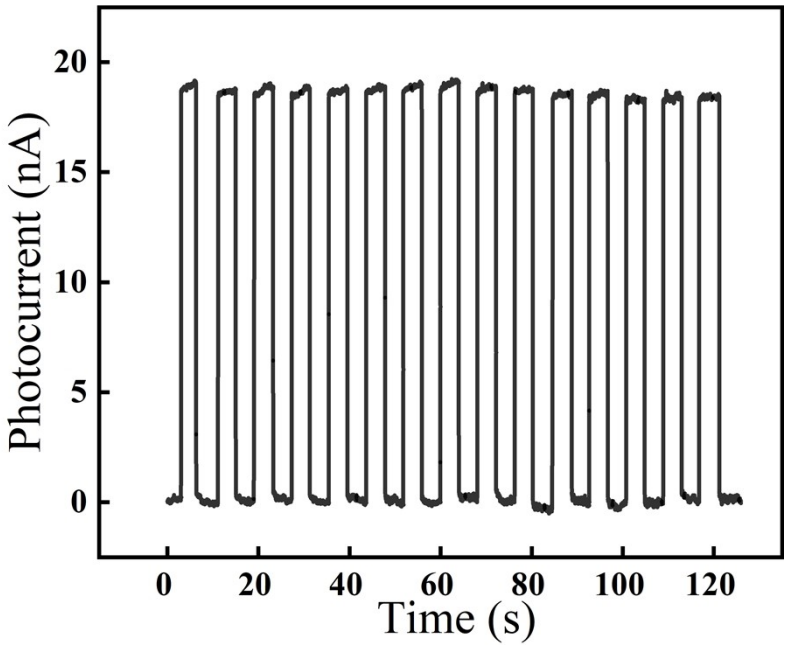

Figure S6. The photodetecting performances of Au-MoS_2 Schottky junction under on/off cycles of 5 mW/cm^2 halogen light.

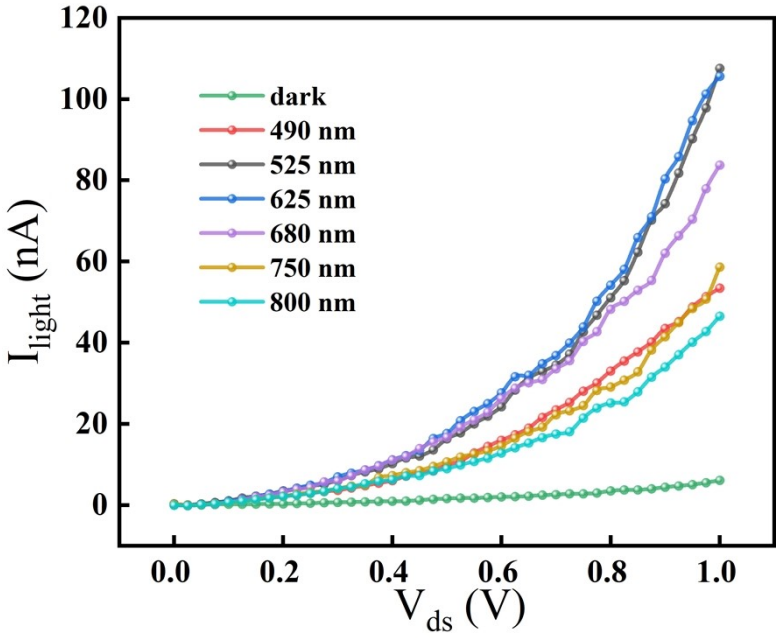

Figure S7. I_{ds}-V_{ds} curves of the Au-MoS_2 Schottky junction when exposed to light at different wavelengths of 1 mW/cm^2 when no bias is applied to NG.

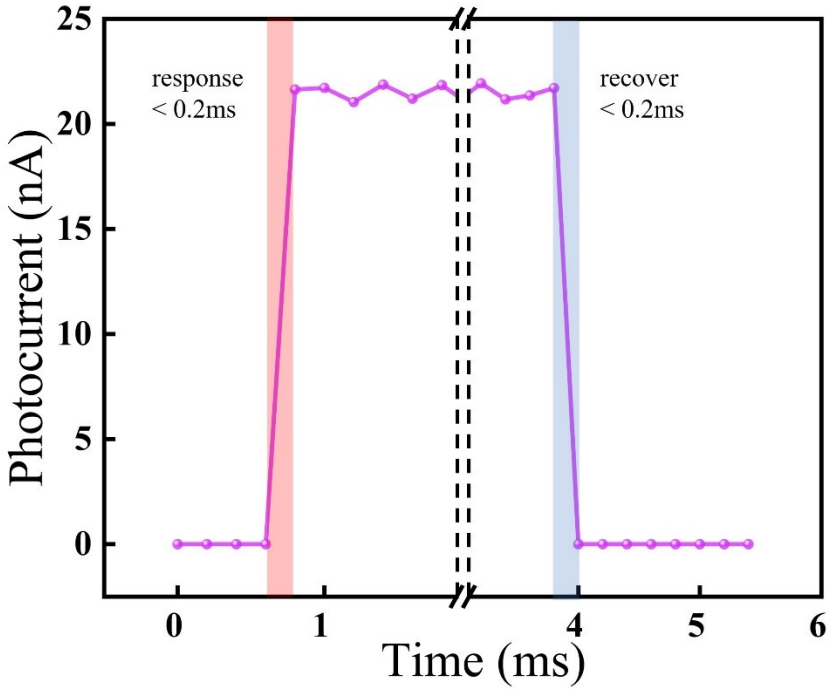

Figure S8. The response and recover speed of the Schottky photodetector.

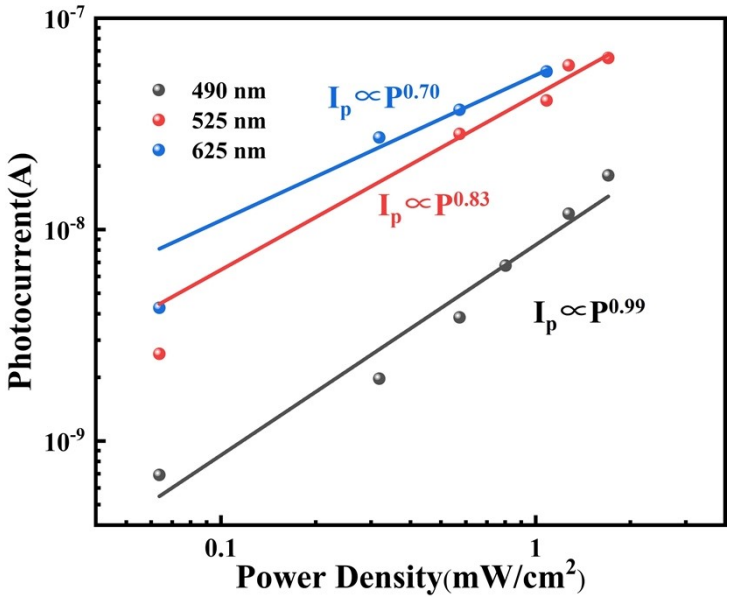

Figure S9. Linearity of the device when the incident light has a wavelength of 490 nm, 525 nm and 625 nm.

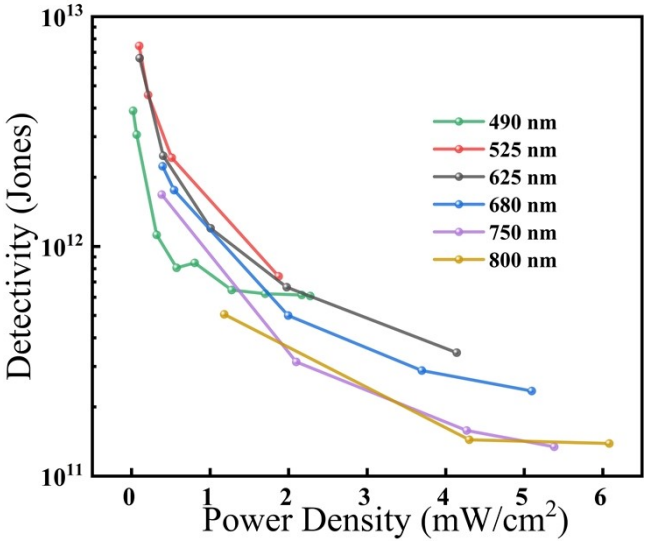

Figure S10. Detectivity under different power density when no NG bias is applied.

6. The simulation of the distribution of light field near the nanowire

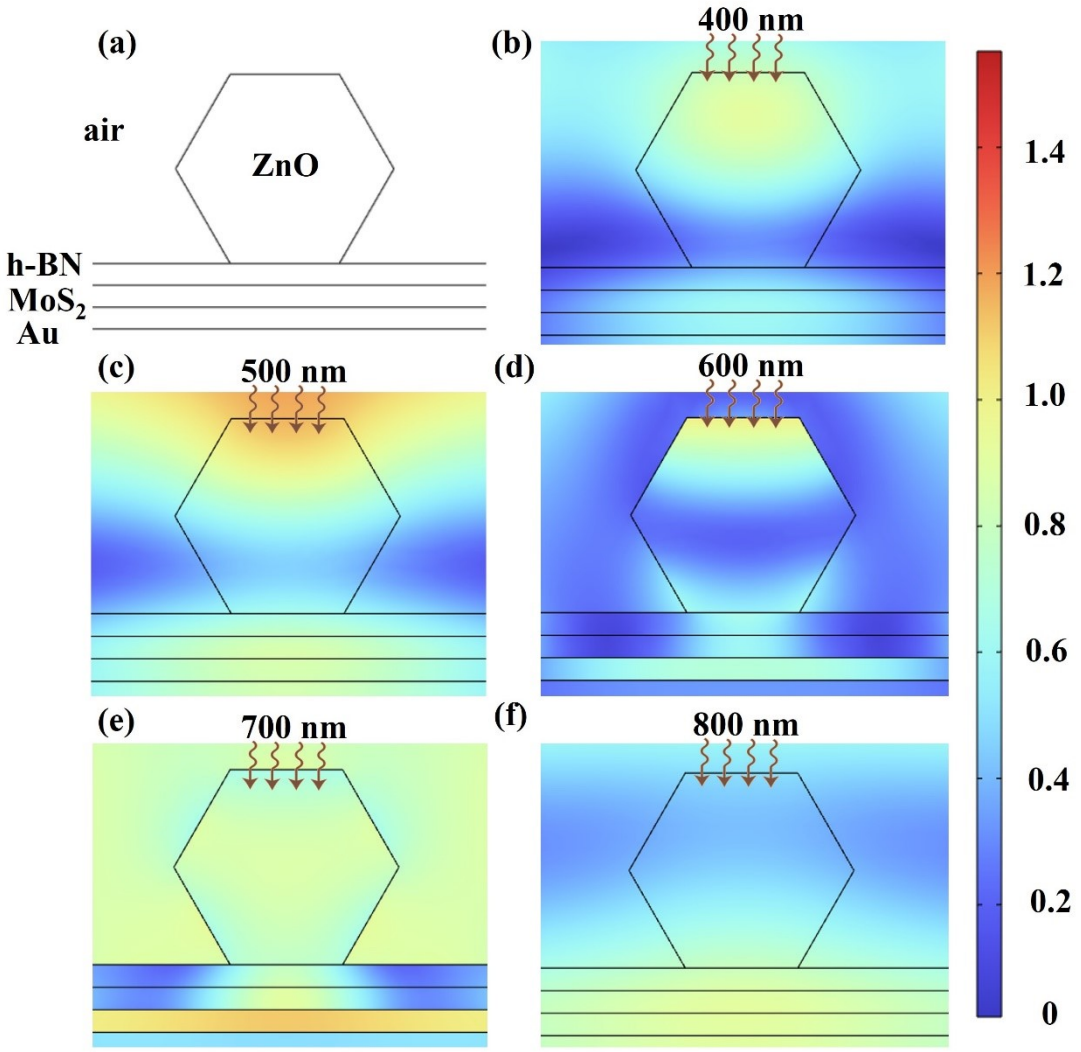

Figure S11. The simulation of the distribution of light field near the nanowire. (a) The basic model of the simulation. (b)-(f) The simulation of the distribution of light field when the incident light is 400 nm (b), 500 nm (c), 600 nm (d), 700 nm (e), 800 nm (f), respectively.

7. The influence region of ZnO nanowire on left side

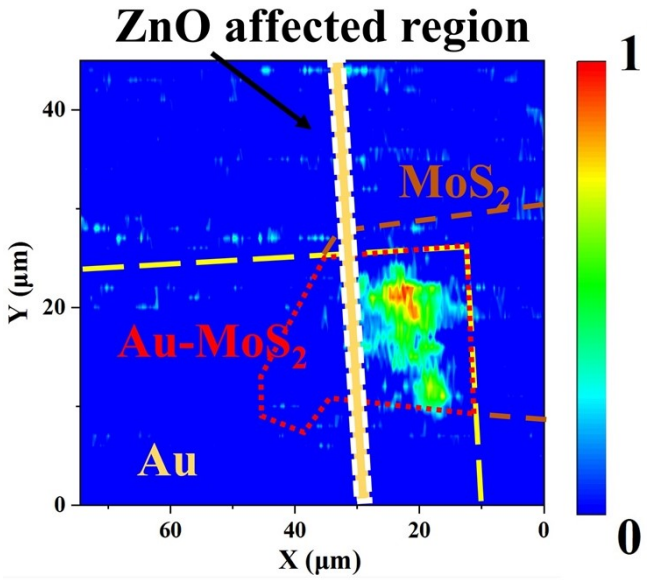

Figure S12. The influence region of ZnO nanowire on left side deviates from the main photocurrent region.

8. The detailed transfer characteristics of the left NG

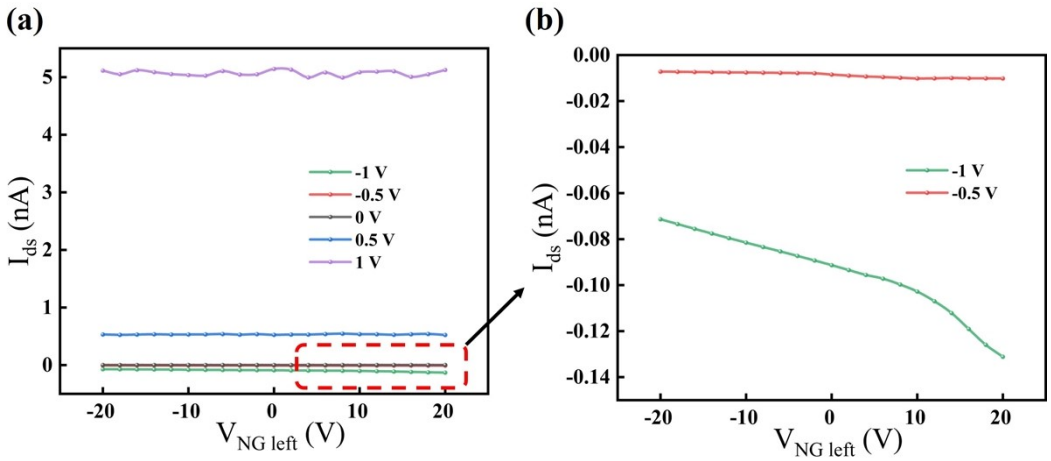

Figure S13. The detailed transfer characteristics of the left NG. (a) The gating effect is not as obvious on the right junction. (b) The red area in (a) is enlarged and the nanowire on the left can gate the left Schottky junction.

II. Supplementary Table

Table1. Comparison of device performances of MoS_2 Schottky based photodetectors.

Schottky Type	**Wavelength (nm)**	**Gate Type**	**V_{ds} (V)**	**Responsivity (A/W)**	**On/off Ratio**	**Detectivity (Jones)**	**Ref**
Au/MoS_2/Au	525/625	nanowire gate (-20V)	1	1.3×10^{2}	6×10^{3}	1.4×10^{13}	**This work**
Au/MoS_2/Au	445	-	10	0.05	-	1.55×10^{9}	**1**
Au/MoS_2/Ti	1310	-	1	1.9	-	2.3×10^{11}	**2**
MoS_2/Pd	488	ion gate (0~-6 V)	1	0.24	1×10^{6}	1.7×10^{11}	**3**
MoS_2/CNT	532	-	1	2.01×10^{3}	-	3.2×10^{12}	**4**
MoS_2/Cr	650	backgate (-60 V)	5	4.10×10^{3}	1.6×10^{2}	1.34×10^{13}	**5**
2H-1T@2H MoS_2	530	backgate (18 V)	20	1.92×10^{3}	-	7.55×10^{11}	**6**
MoS_2/ graphene	432	backgate (-3 V)	0.5	2.2×10^{5}	4×10^{4}	3.5×10^{13}	**7**
MoS_2/$TaIrTe_4$	635	backgate. (-40 V)	1	0.89	1×10^{4}	$\sim9\times10^{11}$	**8**

Reference

1. Y. Xie, B. Zhang, S. Wang, D. Wang, A. Wang, Z. Wang, H. Yu, H. Zhang, Y. Chen, M. Zhao, B. Huang, L. Mei and J. Wang. Ultrabroadband MoS_2 Photodetector with Spectral Response from 445 to 2717 nm. *Adv Mater.* **2017**, *29* (17), 1605972.
2. Y. Mao, P. Xu, Q. Wu, J. Xiong, R. Peng, W. Huang, S. Chen, Z. Wu and C. Li. Self-Powered High-Detectivity Lateral MoS_2 Schottky Photodetectors for Near-Infrared Operation. *Adv. Electron. Mater.* **2021**, *7* (3), 2001138.
3. R. Chang, Q. Chen, W. Shen, Y. Zhang, B. Zhang and S. Wang. Controllable Switching between Highly Rectifying Schottky and p-n Junctions in an Ionic MoS_2 Device. *Adv. Funct. Mater.* **2023**, *33* (30), 2301010.
4. E.-X. Ding, P. Liu, H. H. Yoon, F. Ahmed, M. Du, A. M. Shafi, N. Mehmood, E. I. Kauppinen, Z. Sun and H. Lipsanen. Highly Sensitive MoS_2 Photodetectors Enabled with a Dry-Transferred Transparent Carbon Nanotube Electrode. *ACS Appl. Mater. Interfaces.* **2023**, *15* (3), 4216-4225.
5. Y. Sun, L. Jiang, Z. Wang, Z. Hou, L. Dai, Y. Wang, J. Zhao, Y.-H. Xie, L. Zhao, Z. Jiang, W. Ren and G. Niu. Multiwavelength High-Detectivity MoS_2 Photodetectors with Schottky Contacts. *ACS Nano* **2022**, *16* (12), 20272–20280.
6. I. Lee, W. T. Kang, J. E. Kim, Y. R. Kim, U. Y. Won, Y. H. Lee and W. J. Yu. Photoinduced Tuning of Schottky Barrier Height in Graphene/MoS_2 Heterojunction for Ultrahigh Performance Short Channel Phototransistor. *ACS Nano* **2020**, *14* (6), 7574-7580.
7. W. Wang, X. Zeng, J. H. Warner, Z. Guo, Y. Hu, Y. Zeng, J. Lu, W. Jin, S. Wang, J. Lu, Y. Zeng and Y. Xiao. Photoresponse-Bias Modulation of a High-Performance MoS_2 Photodetector with a Unique Vertically Stacked 2H-MoS_2/1T@2H-MoS_2 Structure. *ACS Appl. Mater. Interfaces.* **2020**, *12* (29), 33325-33335.
8. L. Zhang, X. Han, S. Zhang, H. Wang, Y. Huang, Z. Zheng, N. Huo, W. Gao and J. Li. Gate-Tunable Photovoltaic Behavior and Polarized Image Sensor Based on All-2D $TaIrTe_4$/MoS_2 Van Der Waals Schottky Diode. *Adv. Electron. Mater.* **2022**, *8* (11), 2200551.